Failure Modes and Materials Performance of Railway Wheels

Z.X. Liu and H.C. Gu

(Submitted 1 May 2000)

In this study, the failure modes of cartwheel and mechanical properties of materials have been analyzed. The results show that rim cracking is always initiated from stringer-type alumina cluster and driven by a combination effect of mechanical and thermal load. The strength, toughness, and ductility are mainly determined by the carbon content of wheel steels. The fatigue crack growth resistance is insensitive to composition and microstructure, while the fatigue crack initiation life increases with the decrease of austenite grain size and pearlite colony size. The dynamic fracture toughness, K_{ID}, is obviously lower than static fracture toughness, K_{IC}, and has the same trend as K_{IC}. The ratio of K_{ID}/σ_{YD} is the most reasonable parameter to evaluate the fracture resistance of wheel steels with different composition and yield strength. Decreasing carbon content is beneficial to the performance of cartwheel.

Keywords dynamic fracture toughness, failure analysis, fatigue property, performance evaluation, static mechanical property, wheel steel

1. Introduction

The railway system in China plays a demanding role among all of the methods of transportation (train, motor vehicle, ship, airplane, pipeline, *etc.*). The cartwheel is one of the most critical components in the railway system. A wheel failure can cause a derailment with its attendant loss of life and property. Up to now, high volume cartwheels have been made of 0.47 to 0.8% carbon steel based on pearlite microstructure, and both wrought-steel and cast-steel wheels have been used in China and other countries.

The current trend toward high speed in passenger cars demands prolonging the service life and increasing the reliability of wheels. In order to solve this technical challenge, great efforts to improve the wheel steels have been made. The heat treatment everywhere over the range of cooling rates results in the increase of strength and reduction of ductility with the increase of carbon content in wheel steels. In order to obtain high fracture resistance, the microstructure uniformity and pearlite dispersity must be raised.[1–6] The increase of carbon content, especially in the range of 0.45 to 0.65%, will increase the thermal cracking trend, which will increase the flat possibility.[7]

In the present investigation, the main failure modes of cartwheel, especially rim cracking, were analyzed. The mechanical properties of six kinds of wheel steels used in China with different carbon content and processing were measured. Their effect on performance of cartwheel was analyzed.

Z.X. Liu and **H.C. Gu**, State Key Laboratory for Mechanical Behavior of Materials, Xi'an Jiaotong University, Xi'an, 710049, People's Republic of China. Contact e-mail: hcgu@xjtu.edu.cn.

2. Materials and Experimental Procedure

Ma Anshan Iron and Steel Company Ltd. (Ma Anshan City, East China) supplied the experimental materials used in the mechanical properties test. The chemical composition of materials is presented in Table 1. For comparison, all specimens were cut from the rim part of real wheels at the same position. The failure specimens were analyzed with a Hitachi S-2700 type scanning electron microscope (SEM). The microstructure parameters were determined by quantitative metallography technology. The composition of inclusions in crack initiation sites was analyzed by x-ray energy dispersive spectrum analysis in the SEM. The static mechanical properties (strength and plasticity) were measured using smooth samples of 10 mm diameter and 50 mm gauge length. The static fracture toughness, K_{IC} (actually, K_Q), and fatigue properties (fatigue crack initiation life, N_i, and fatigue threshold value, ΔK_{th}), were measured with a single edge notch sample, with dimensions of 12.5 × 25 × 120 mm, and a notch with depth of 1.5 mm and radius of 0.2 mm, on an Instron tester and an Amsler HFP5100 high frequency fatigue tester, respectively. The impact toughness, a_k, and dynamic fracture toughness, K_{ID}, were measured using standard Charpy U-notch and precracked Charpy V-notch samples with dimensions of 10 × 10 × 55 mm, on a JBC-3000 instrumented impact tester with a total energy of 300 J and a load rate of 5 m/s, respectively. The dynamic fracture toughness K_{ID} and dynamic yield strength σ_{YD} were calculated according to Ref 8.

3. Results and Discussion

3.1 Failure Analysis

The major failure modes of railway wheel can be classified into five types: shelling, spalling, flat, rim cracking, and brittle fracture. The brittle fracture of wheels occurs very infrequently and can be prevented by regular quality control (compositional analysis, mechanical testing, and physical inspection). If brittle fracture occurs on only one wheel, then all wheels made of the

Fig. 1 Fractography surface of rim cracking

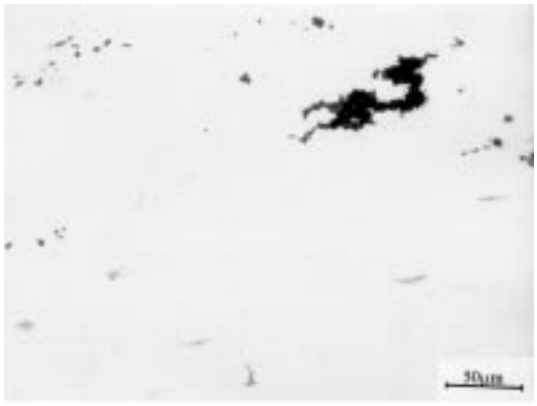

Fig. 2 Inclusion shape near crack initiation site

Table 1 The composition of wheel steels (wt.%)

Sample	Process state	C	Si	Mn	S	P
R1	Rolling	0.51	0.24	0.7	0.011	0.012
R2	Rolling	0.55	0.28	0.73	0.01	0.01
R3	Rolling	0.60	0.31	0.85	0.012	<0.01
R4	Rolling	0.62	0.22	0.69	0.021	0.022
C1	Casting	0.66	0.46	0.78	0.021	0.015
C2	Casting	0.68	0.45	0.75	0.02	0.02

Table 2 The statistical distribution of inclusions across the wheel section

Distance beneath tread	<30 mm	30 to 50 mm	50 to 60 mm
Inclusion number	27	13	1
%	67	32	1

same heat steel must be removed from service. Shelling, spalling, and flat are three trifling damage modes. The shelling is an irregular loss of metal from a tread surface of about 1 to 3 mm. The fatigue crack may be initiated by heavy deformed pearlite fragment, brittle inclusion located in the maximum reversed contact stress region or by the breakage of martensite caused by braking.[9,10] Spalling also stems from rolling contact fatigue, but the metal is removed in the form of pitting from the tread surface. A flat is likely to occur when the wheel is locked in a car that is running and while the contact point of tread is skidding on the rail. These three damages can be removed from the tread by machining for a reprofile of the wheel edge. An increase in strength and hardness of the wheel can effectively decrease the occurrence of shelling, spalling, and flat.

The rim cracking is a fatigue process and may be the most dangerous failure mode, for there is no prior indication of impending disaster. It is usually nucleated inside the rim and is invisible until the crack has grown to a lateral surface. If the crack grows to the critical length, then a broken piece will fall. Figure 1 shows the macroappearance of a broken piece. The beach marks are evident on the fracture surface. These markings are attributed to the movement of two crack surfaces that open, close, and rub together during loading.

The distinct crack initiation site always accompanies the stringer-type alumina cluster over 0.5 mm in size. Figure 2 shows the inclusion near the crack initiation site. These inclusions are composed of Al_2O_3 plus $6Al_2O_3 \cdot CaO$, and, sometimes, duplex inclusions MnS plus Al_2O_3 are also found. Table 2 gives the statistical result of naked eye inclusion distribution across the cartwheel section selected from 38 sets of failed wheels. The larger inclusion is mainly distributed within the 30 mm beneath the tread of the cartwheel, which corresponds to the occurring position of rim cracking. During heat treatment, higher tension stress will be produced on the interface of the inclusion and matrix after cooling, because there is a large difference between the inclusion and matrix in the elastic module and thermal expansion coefficient. The inclusions detach from the matrix or fracture to form voids under the contact stress. This detachment or voids of inclusions can be considered as a defect or microcrack. It is easy for rim cracking to initiate from them under the effect of maximum shear stress.

The peak values of cycle stress amplitudes calculated by the Hertzian rolling pressure are located at about 1 to 3 mm beneath the tread/rail contact surface, which is much less than the measurement at which the rim cracking occurs, so it is impossible that the fatigue crack growth is only driven by mechanical loads. It has been reported previously that the thermal stresses created by braking are many times larger than the stresses induced by mechanical loads. These thermal stresses in the rim would provide the driving force for fatigue crack propagation.[11] Our results measured by the drilling method and x-ray method, with consecutive corrosion to denude the surface layers, show that the high values of residual tensile stresses, 57.9 MPa in the radial direction and 49.6 MPa in the circumferential direction, exist below the contact surface in a broken piece cut from failed cartwheel. Therefore, the driving force of the fatigue crack must be the combination effect of mechanical load and thermal load.

3.2 Mechanical Properties

Figure 3 and 4 show the mechanical and fatigue testing results of six kinds of wheel steels. The ductility (elongation),

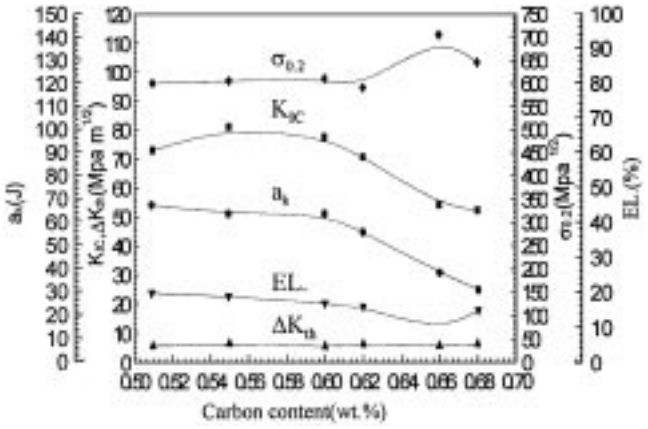

Fig. 3 Influence of carbon content on mechanical properties

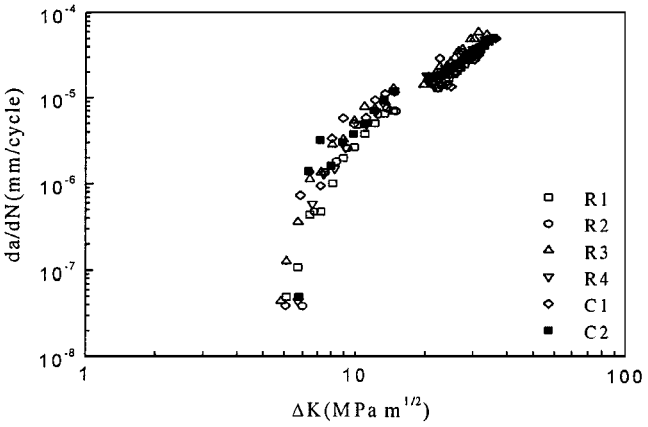

Fig. 4 *da/dN*-Δ*K* curves of the wheel steels

impact toughness (a_k), and fracture toughness (K_{IC}, actually K_Q) increase, while the strength (yield strength, $\sigma_{0.2}$, and tensile strength) decreases as the carbon content decreases. However, the fatigue crack growth rates in the Paris regime and fatigue thresholds (ΔK_{th}) were found to be insensitive to composition and microstructure. It is noticeable that despite the variation in carbon content and manufacture process, it seems that the fatigue crack initiation life (N_i) increases with the refinement of austenite grain and pearlite colony (Fig. 5).

It has been shown in a previous investigation on fully pearlitic steels that the strength is determined by cementite interlamellar spacing, while the toughness and ductility are determined by austenite grain size.[1–6] In this investigation, the mechanical properties of wheel steels are found to be affected by composition as well as microstructure. The prior austenite grain size and cementite interlamellar spacing are about 8 to 19 μm and 0.12 to 0.13 μm, respectively. The effect of difference of microstructure parameters among materials tested on mechanical properties is less marked than that of carbon content.

The resistance of fatigue crack growth is affected by the effective grain size (or fatigue crack growth mean free path between two obstructors), such as ferrite grain size for low carbon steels or pearlite colony size for pearlitic steels.[12,13] The *in-situ* observation results showed that the fatigue crack

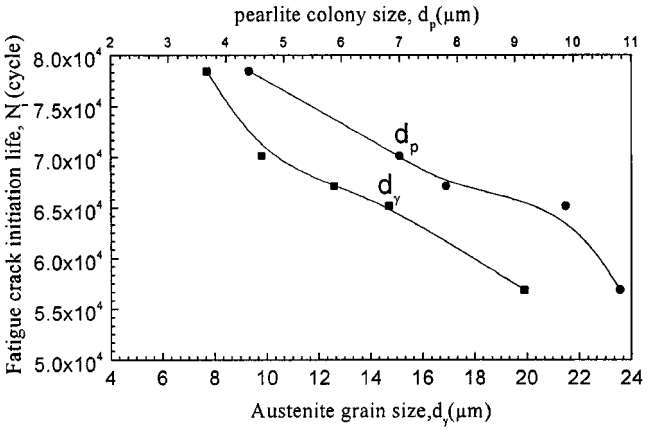

Fig. 5 Influence of austenite grain side $d\gamma$ and pearlite colony size d_p on fatigue crack initiation life N_i

could propagate along or cross ferrite grain and cementite lamella in wheel steels. The meandering at the grain boundary and pearlite colony boundary was obvious, but the meandering probability was different in different materials, which is mainly related to ferrite distribution along the grain boundary. Because the carbon content and treatment process were different, the ferrite distributed on the grain boundary in materials R1, R2, and R4 was continuous and thick, but that in R3, C1, and C2 was discontinuous and thin. The probability of fatigue crack meandering in the former was larger than that in the latter at the grain boundary, while the reverse regulation was observed at the pearlite boundary. It is clear that the effective grain size cannot be determined only in terms of pearlite colony or austenite grain size. It depends on the probability of fatigue crack meandering at the grain boundary and pearlite colony boundary. The value of the effective grain size may be approach the grain size for materials with a continuous ferrite network, while it may approach to the pearlite colony size for the materials with discontinuous ferrite network, which produces the results that the wheel steels with different austenite grain size and pearlite colony size almost have the same effective grain size and resistance of fatigue crack growth. However, coarsing austenite grain makes large inclusions, which unevenly distribute on the grain boundaries and reduce the join strength of the boundary. The examination of inclusions has validated that the larger block inclusions always distribute on grain boundaries. So the possibility of fatigue crack initiated by inclusion breaking and by boundary debonding will increase. It is not surprising that the fatigue crack initiation life is sensitive to austenite grain size and pearlite colony size.

Figure 6 shows the relation of dynamic fracture toughness, K_{ID}, versus carbon content at different temperatures. The values of K_{ID} are obviously lower than those of K_{IC} and have the same trend as K_{IC} (comparing Fig. 5 with Fig. 6 at room temperature), but the difference in these parameters among materials decreases. The dynamic fracture toughness represents the cracking resistance of materials at high load rate. At high load rate, the dislocation thermal activation process is restrained, which results in the decrease of dislocation mobility in ferrite and the rise of yield strength of ferrite. Therefore, the plastic relaxation

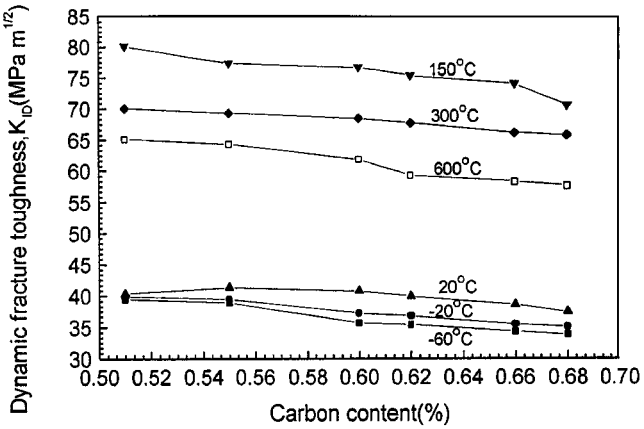

Fig. 6 Influence of carbon content on dynamic fracture toughness at different temperature

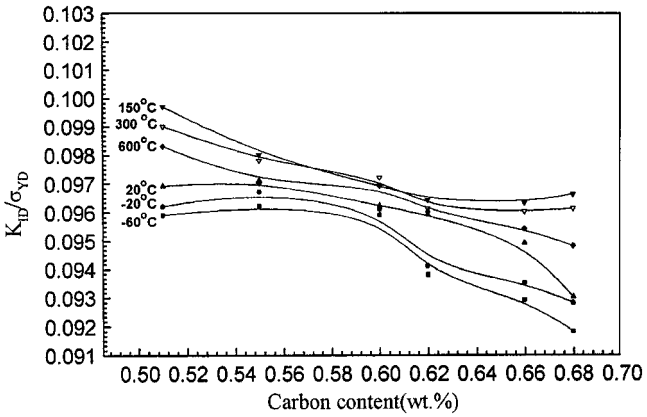

Fig. 7 The ratio of K_{ID}/σ_{YD} of wheel steels at different temperatures

at the crack tip decreases and the cracking of carbides is promoted. The microcrack can be initiated and grown by consuming less energy, which leads to the decrease of crack growth resistance. This effect is especially obvious for the medium and high carbon steels used in the cartwheel. That is, the dynamic fracture toughness K_{ID} is observably lower than the static fracture toughness K_{IC}, and the difference of K_{ID} among materials decreases.

4. Synthetic Evaluation of Performance

To evaluate the difference of fracture resistance among wheel steels, it is improper only to use the fracture toughness (K_{IC} or K_{ID}). The critical crack size a_c of wheel steels used in the cartwheel can be calculated as follows:

$$a_c = (YK_{IC}/\sigma_C)^2 \qquad \text{(Eq 1)}$$

where Y is the crack geometry factor, which equals to 1.1, 0.69, and 0.5, corresponding to surface cracks, corner cracks, and through-thickness edge cracks, respectively; and σ_c is the fracture strength that relates to yield strength. If σ_c in Eq 1 is replaced by σ_{YD} or $\sigma_{0.2}$, the ratio of K_{ID}/σ_{YD} or $K_{IC}/\sigma_{0.2}$ is approximately proportional to $a_c^{1/2}$. The steels with the same ratio will have the same fracture resistance even though they have different values of yield strength and fracture toughness. Figure 7 shows the ratio of K_{ID}/σ_{YD} of different materials at all testing temperatures. It can be found that the ratio of K_{ID}/σ_{YD} decreases with the raise of carbon content. Comparing Fig. 7 with Fig. 6, the beneficial effect of lowering carbon content on the fracture resistance evaluated by the ratio of K_{ID}/σ_{YD} is more obvious than that evaluated only by K_{ID}.

It is clear that the wheel steels with lower carbon content have excellent combination of strength and plasticity and higher fracture resistance, which will effectively decrease the occurrence of brittle fracture event.

Furthermore, considering the fact that almost all rim crackings are nucleated from Al_2O_3 or $6Al_2O_3 \cdot CaO$ inclusions, it is necessary using secondary steelmaking to produce "clean" steel. Ladle injection, by which a special deoxidizer and rare earth metals were added to the ladle, was an effective process for achieving good inclusion morphology. SEA-SKF equipment, the induction stirring-arc reheating system, is being used for degassing and desulfurizing of wheel steels in China nowadays.

The wrought wheels made of R1 steel have been used in some lines running at accelerated speed. According to calculation, the mechanical load will increase twofold at higher speed than before. Nevertheless, it seems that employing a more severe quenching method to the wheel tread is necessary to raise its abrasion resistance.

5. Conclusions

- The failure modes of cartwheel are shelling, spalling, flat, and rim cracking. The microcrack of rim cracking is usually initiated from stringer-type alumina cluster. The driving force of fatigue crack growth is supplied by a combination effect of mechanical and thermal loads.
- The ductility, impact toughness, and fracture toughness increase, while the strength decreases with the decrease of carbon content. The fatigue crack growth resistance is insensitive to the variation of composition and microstructure, but the fatigue initiation life increases with refinement of austenite grain and pearlite colony.
- The dynamic fracture toughness is lower than static fracture toughness. The difference in dynamic fracture toughness among materials decreases compared with that of static fracture toughness in the range of testing temperatures.
- The ratio of K_{ID}/σ_{YD} may be a reasonable parameter for evaluating the fracture resistance for wheel steels.

Acknowledgments

The authors gratefully acknowledge Ma Anshan Iron and Steel Company Ltd., for providing testing material, and The State Key Lab for Mechanical Behavior of Materials, Xi'an Jiaotong University, for providing laboratory facilities, in which this work was carried out, and for financial support.

References

1. A.R. Rosenfield, G.T. Hahn, and J.D. Embury: *Metall. Trans. A*, 1972, vol. 3A, pp. 2797-2804.
2. F.P.L. Kavishe and T.J. Baker: *Mater. Sci. Technol.*, 1986, vol. 2(6), pp. 583-88.
3. Y.J. Park and I.M. Bernstein: *Metall. Trans. A*, 1979, vol. 10A, (11), pp. 1653-64.
4. J.J. Lewandowski and A.W. Thompson: *Metall. Trans. A*, 1986, vol. 17A, pp. 461-72.
5. J.M. Hyzak and I.M. Bernstein: *Metall. Trans. A*, 1976, vol. 7A, pp. 1217-24.
6. F.P.L. Kavishe and T.J. Bakler: *Mater. Sci. Technol.*, 1986, vol. 2 (8), pp. 816-22.
7. Kigawa Takehiko and Kimoto Eiji: "Evaluation of the Flat-Resistance Property of Wheel Materials," Quarterly Report of RTRI (Railway Technical Research Institute), RTRI, Tokyo, Japan, 1990, vol. 31(2), pp. 104-08.
8. W.L. Server: *J. Test. Eval.*, 1978, vol. 6 (1), pp. 29-34.
9. J. Kalousek, E. Magel, J. Strasser, W.N. Caldwell, G. Kanevsky, and B. Blevins: *Wear*, 1996, vol. 191, pp. 210-18.
10. R. Lunden: *Wear*, 1991, vol. 144, pp. 57-70.
11. M.R. Haley, H.R. Larson, and D.G. Kleeschulte: *J. Eng. Mater. Technol.*, 1980, vol. 102 (1), pp. 26-31.
12. G.R. Yoder, L.A. Cooley, and T.W. Crooker: *Fracture Mechanics: Four Symposium Vol I: Theory and Analysis*, ASTM STP 791, J.C. Lewis and G. Sines, ASTM, Philadelphia, PA, 1983, pp. 348-65.
13. D. Taylor: *Fatigue Thresholds*, Butterworth and Co. (Publishers) Ltd., London, 1989, pp. 71-92.